

SATELLITE ORBIT UNDER INFLUENCE OF A DRAG - ANALYTICAL APPROACH

M. M. Martinović and S. D. Šegan

*Department of Astronomy, Faculty of Mathematics, University of Belgrade,
Studentski trg 16, 11000 Belgrade, Serbia*

E-mail: mihailo.martinovic@obspm.fr

(Received: March 15, 2017; Accepted: August 2, 2017)

SUMMARY: The report studies some changes in orbital elements of the artificial satellites of Earth under influence of atmospheric drag. In order to develop possibilities of applying the results in many future cases, an analytical interpretation of the orbital element perturbations is given via useful, but very long expressions. The development is based on the TD88 air density model, recently upgraded with some additional terms. Some expressions and formulae were developed by the computer algebra system Mathematica and tested in some hypothetical cases. The results have good agreement with iterative (numerical) approach.

Key words. Atmospheric effects – Celestial mechanics

1. INTRODUCTION

A satellite orbiting around an isolated spherical planet with no atmosphere would indefinitely follow the same elliptic orbit, without any variation of the trajectory. However, for the case of real Earth this simple picture is greatly altered by perturbing forces, usually classified into two major groups:

- (i) Perturbations of the total gravity field that acts on the satellite. These effects can appear due to gravitational attraction of Sun and Moon (gravity effects of other celestial bodies are negligible), but also as a result of the variation of Earth's gravitational attraction, caused by flattening at the poles and other departures from spherical symmetry, such as the "pear-shape" effect. When analyzing satellite dynamics, the total gravity perturbation is considered to be the sum of all particular contributions, independent on the satellite mass, size or geometry.
- (ii) Non-gravitational effects, proportional to the area-to-mass ratio of the satellite. Here we primarily consider the air drag, caused by rapid

movement of a satellite through the upper atmosphere, but also effects of the solar radiation pressure.

For most satellites, these are two types of force that induce major perturbations in the orbits. Many other perturbations exist, but do not normally produce large changes and will therefore be ignored here, as we aim to provide basic description. These neglected perturbations appear, among other causes, due to: upper-atmosphere winds, solar radiation reflected from Earth, Earth tides and ocean tides, precession of the Earth's axis in space, resonance with Earth's gravitational field and relativity effects. Although these effects will be ignored, it should be noted that they can be important for some special satellites.

Parameters of the satellite orbit and its motion are given in Table 1. Several elements in the table are not self-explanatory. First, the drag coefficient C_d is a parameter that describes aerodynamic properties and is determined by the satellite geometry. The model for calculation of this coefficient, which would widely be accepted in the community, still does not exist. Values in the interval 2.1-2.3 were obtained for spherical satellites by most of the

Table 1. Notation. Values of the scale height and model constants are given on the attached link, along with derived Equations

Symbol	Meaning	Unit / Value
a	Semi-major axis	km
e	Eccentricity	
i	Inclination	rad
ω	Argument of perigee	rad
n_{sc}	Satellite mean motion	rad/day
m_{sc}	Satellite mass	kg
S_{sc}	Satellite cross-section	m^2
C_d	Drag coefficient	2.2
t	Local stellar time	rad
d	Day of year	rad
ν	Mean anomaly	rad
E	Eccentric anomaly	rad
α_\odot	Right ascension of the Sun	rad
Ω	Right ascension of the ascending node	rad
φ	Declination of the satellite	rad
F_b	Solar flux at $\lambda = 10.7\text{cm}$	$10^{-22}Wm^{-2}Hz^{-1}$
F_x	81-day average of F_b	$10^{-22}Wm^{-2}Hz^{-1}$
K_p	Planetary K index 3h before observation	
ω_t	Angular velocity of thermosphere	$2\pi \text{ rad/day}$
ϵ	Flattening of Earth	0.00335
R_\odot	Radius of Earth	6371km
h_0	Base of the heterosphere	120km
H	Scale height	km
K, p_n, a_n	Constants of the model	

previous authors (see e.g. Bezdek and Vokrouhlický 2004). We will use the constant value of $C_d = 2.2$ further on, while more accurate predictions of the drag coefficient for cubical satellites and satellites with solar panels will be provided in next installment of this article. Second, the planetary K_p index illustrates the magnitude of geomagnetic storms, being an excellent indicator of disturbances in the Earth's magnetic field. It takes values from 0 to 9 by convention, increasing logarithmically with strength of a storm. We use geocentric reference system, also assuming that the thermosphere is corotating with Earth. This approximation is widely used in modeling of the atmosphere (Milani et al. 1987), although the level of its validity can be questioned at higher altitudes. The scale height H is the altitude increase for which the total density changes e_c times, where $e_c \approx 2.71$ is Euler's number.

The upper atmosphere is extremely rarefied, having a density of about 10 g/cm^3 at a height of 350 km. However, a satellite travels at nearly 8 km/s, so its collisions with air molecules are frequent enough to create an appreciable drag force. If the orbit is non-circular, the air drag is much greater at perigee than at apogee, and the effect of the drag on the orbit is to retard the satellite at perigee, so it doesn't fly out so far at apogee. Consequently, the orbit contracts and tends to become circular, but the perigee height decreases very slowly. In terms of the orbital elements a, e, i, Ω and ω , the air drag reduces both

a and e , but $a(1 - e)$ is an almost constant value. The effect on the other three elements is indirect; for example, the rate of change of Ω is dependent on a and increases as a decreases. If the orbit is initially circular, air drag acts all round the orbit, reducing height of the satellite gradually and causing it to slowly spiral inwards.

For both circular and elliptic orbits, the drag rapidly increases as perigee height decreases. When perigee descends to about 100 km, the satellite can no longer remain in the orbit, and begins its final plunge into the lower atmosphere. It should be noted that although air drag retards the satellite at perigee, its overall effect is to make the satellite travel faster. The orbital period decreases as its lifetime proceeds, and the final decay usually occurs when the orbital period has fallen under about 90 minutes.

In this preliminary report, we provide insights in the analytical method that describes evolution of the satellite orbit parameters without using complicated numerical integrations characteristic for the treatment of the thermosphere density models. Work with similar aim was done before by Šegan (1988), but was limited only to zero-eccentricity orbits. After briefly introducing the method in Section 2 we elaborate it in detail in Section 3, while the obtained results are shown and discussed in Section 4. Plans and "roadmap" for providing an interactive online interface that would make this model easily applicable and available to the community is given in Section 5, along with some general conclusions.

2. EFFECTS OF THE AIR DRAG

The computation of drag effects in the motion of an artificial satellite is performed by the method of variation of elements. Changes are expressed by Lagrange's equations of motion in Gauss' form (King-Hele 1987). Usage of canonical elements has here limited validity since mathematical description of the air density must be in a very simple form.

Lagrange equations for perturbations over one revolution lead to an integrable system of differential equations. Complications arise from complexity of expressions for the air density. Usage of the aeronomic models (CIRA, MSIS ... see e.g. Vallado 2010) is impossible for such analytical work since the mathematical description of the air density is very complicated and each atmospheric constituent must separately be discussed.

On the heights which are most important for our study, i.e. 150-1200 km perigee heights, the surfaces of constant density tend to be spheroidal with approximately the same ellipticity as solid Earth. Therefore, we assume that for any geocentric latitude air density varies exponentially with attitude.

3. THE METHOD USED

We are taking the Sehnal's (1986) method for approximation of the atmospheric total density distribution, using linearized form of spherical function representation:

$$\rho = \sum_{j=1}^3 \rho_s^{(j)} e^{\frac{h_0-h}{jH}} = \sum_{j=1}^3 \sum_{n=1}^7 A_n^{(j)} f_n e^{\frac{h_0-h}{jH}}, \quad (1)$$

where $A_i^{(j)}$ expresses the geometry while f_i are functions of physical parameters.

Formulation of upgraded Sehnal's model is given as (see e.g. Marčeta and Šegan 2010 for details):

$$\rho = f_x f_0 k_0 \sum_{n=1}^7 h_n g_n, \quad (2)$$

where:

$$f_x = 1 + a_1(F_x - F_b),$$

$$f_0 = a_2 + f_m,$$

$$f_m = (F_b - 60)/160,$$

$$k_0 = 1 + a_3(K_p - 3).$$

Solar and geomagnetic effects are included through g_n functions, given by following expressions:

$$g_1 = 1,$$

$$g_2 = f_m/2 + a_4,$$

$$g_3 = (a_5 f_m + 1) \sin(d - p_4),$$

$$g_4 = (a_6 f_m + 1) \sin 2(d - p_5),$$

$$g_5 = \sin(d - p_3) \sin \varphi,$$

$$g_6 = (a_7 f_m + 1) \sin(t - p_6) \cos \varphi,$$

$$g_7 = (a_8 f_m + 1) \sin 2(t - p_7) \cos^2 \varphi.$$

Here, for $n = 5 - 7$ we can separate the "quasi-stationary" part \bar{g}_n , being the terms that depend on the solar flux and are considered constant during one revolution, and "periodical" terms \tilde{g}_n that describe local time and declination effects.

The dependence on height is given in detail by Bezdek and Vokrouhlický (2004). Here, we reproduce only the expression used for derivation of the analytical model:

$$h_n = K_{n0} + \sum_{j=1}^3 K_{nj} B_j \Psi_j(E) e^{z_j \cos E}, \quad (3)$$

with $z_j = ae/jH$ and:

$$\begin{aligned} \Psi_j &= e^{c_j \cos(2(u))} \approx 1 + c_j \cos(2(\omega + E)) \\ &+ \frac{1}{4} c_j^2 [1 + \cos(4(\omega + E))] + ec_j [\cos(2(\omega + E) + E) \\ &- \cos(2(\omega + E) - E)] \dots \end{aligned}$$

where $u = \omega + \nu$. Expansion up to the second order of the small term:

$$c_j = \frac{\epsilon R_\odot}{2jH} \sin^2 i$$

is performed. The term that depends on altitude is given as:

$$B_j = e^{\frac{h_0 + R_E - a}{jH} - c_j}.$$

As the density model is fully defined, we further give the expression for the change in the semi-major axis during one revolution (see e.g. King-Hele 1964):

$$\Delta a = -a^2 \delta \int_0^{2\pi} \Sigma_a \rho dE \quad (4)$$

where we introduce:

$$\delta = C_d S_{sc}/m_{sc},$$

$$\Sigma_a = \beta^2 F_+ \sqrt{F_+/F_-},$$

$$\beta = 1 - \tau F_-/F_+,$$

$$\tau = (\omega_t/n_{sc}) \sqrt{1 - e^2} \cos i,$$

$$F_\pm(E) = 1 \pm e \cos E.$$

From the results of the same authors we can investigate the evolution of eccentricity and inclination as:

$$\Delta e = -a\delta \int_0^{2\pi} \Sigma_e \rho dE,$$

$$\Sigma_e = \frac{n^2 \cos E}{F_+} \Sigma_a + \frac{e\tau}{2} \beta F_- \sqrt{\frac{F_-}{F_+}} \sin^2 E,$$

$$\begin{aligned}\Delta i &= -a\delta \frac{\tau \operatorname{tg} i}{2\eta^2} \int_0^{2\pi} \Sigma_i \rho dE, \\ \Sigma_i &= \beta F_-^2 \sqrt{F_+ F_-} \cos^2 u, \\ \eta &= \sqrt{1 - e^2}.\end{aligned}$$

However, the analysis of Δe and Δi in analytical form is outside of the scope of this paper and will be provided during the future work. Here, we analyze Δa by following the satellite revolution as evolution of the eccentric anomaly over a complete circle. Factors t and φ that appear in \tilde{g}_n can be derived as functions of E using the basic spherical trigonometry:

$$\begin{aligned}\sin \varphi &= \sin i \sin u, \\ \sin t \cos \varphi &= \cos(u) \sin(\Omega - \alpha_{\odot}) \\ &\quad + \sin(u) \cos(\Omega - \alpha_{\odot}) \cos i, \\ \cos t \cos \varphi &= \cos(u) \cos(\Omega - \alpha_{\odot}) \\ &\quad - \sin(u) \sin(\Omega - \alpha_{\odot}) \cos i,\end{aligned}$$

to finally obtain:

$$\begin{aligned}\Delta a &= -2\pi a^2 \delta f_x f_0 k_0 \\ &\left[\sum_{n=1}^4 g_n \left(K_n U + \sum_{j=1}^3 B_j K_{nj} U_j \right) \right. \\ &\quad \left. + \sum_{n=1}^4 \bar{g}_n \left(K_n V_n + \sum_{j=1}^3 B_j K_{nj} V_j \right) \right], \quad (5)\end{aligned}$$

where:

$$\begin{aligned}U &= \frac{1}{2\pi} \int_0^{2\pi} \Sigma_a dE, \\ U_j &= \frac{1}{2\pi} \int_0^{2\pi} \Sigma_a \Psi_j e^{z_j \cos E} dE, \\ V_n &= \frac{1}{2\pi} \int_0^{2\pi} \tilde{g}_n \Sigma_a dE, \\ V_{nj} &= \frac{1}{2\pi} \int_0^{2\pi} \tilde{g}_n \Sigma_a \Psi_j e^{z_j \cos E} dE.\end{aligned}$$

Analytical expressions are obtained by expanding Eq. 5 in series for small arguments e , c_j and τ . In this work, the series is expanded up to the second order of each of the small factors. The results are not given here due to their length, but are rather given at http://www.das.org.rs/documents/SAJ_2017_EAD.pdf.

4. SOME PROPERTIES OF THE MODEL

The model provided in Section 3 is established as an algorithm with multiple input parameters that gives a value of Δa as output. In order to validate the method and investigate some of its most important features, we illustrate the variation of Δa as function of particular input parameters. Results are given in Figs. 1-8. At each of figures, the parameters which are not varied are fixed to the following values: $a = 6.7 \cdot 10^3$ km, $e = 0.04$, $i = 5\pi/12$, $\omega = \pi/7$, $\Omega = \pi/12$, $\alpha = \pi/13$, $n_{sc} = \pi/7$, $F_b = 70$, $F_x = 72$, $K_p = 1$, $d = 220 \cdot 2\pi/365.25$.

In Fig. 1 we see the expected result of the atmospheric drag effect exponentially decreasing with altitude due to exponential decrease in the total density. On the other hand, the minimal variation of a with inclination is for $i \sim \pi/2$ (Fig. 2), which is a direct consequence of the Earth flattening near poles. The same effect is visible in Fig. 3 for $\omega \sim \pi/2$, as the orbit shape tends to "follow" the planet shape.

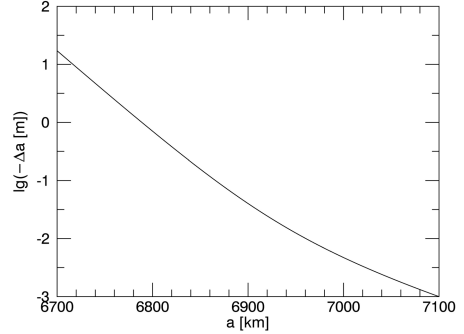


Fig. 1. Change of the semi-major axis dependent on its initial value.

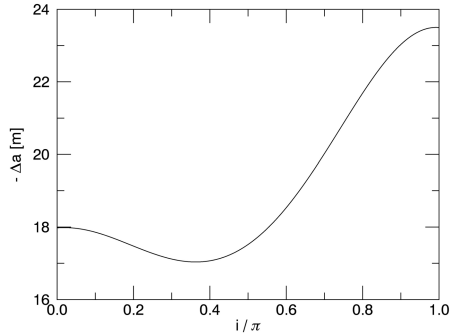


Fig. 2. Change of the semi-major axis with inclination.

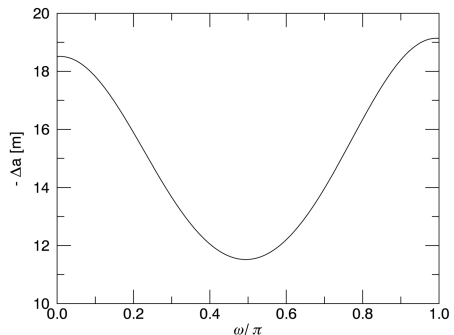


Fig. 3. Change of the semi-major axis with argument of perigee.

An interesting feature to analyze is the behavior of Δa with the current value of the solar flux given in Fig. 4. Namely, the effect of the atmospheric drag scales, roughly linearly, with the absolute value of $F_x - F_b$ shifted by a certain factor. This effect originates from the f_x term that describes solar activity, and has been recently studied in detail by Khalil and Samwel (2016).

As already noted in Section 1, the atmospheric drag is increasing the value of n_{sc} as the mission progresses. In Fig. 5 we can clearly observe the catastrophic decrease in altitude as the orbital period $T = 2\pi/n_{sc}$ falls under the certain value. This

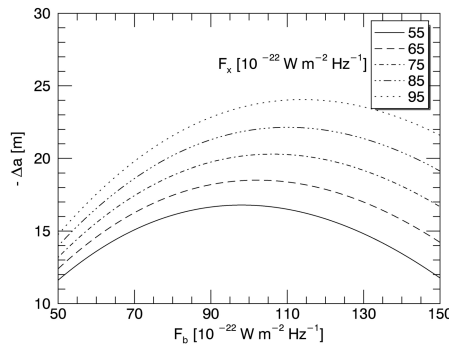


Fig. 4. Change of the semi-major axis with solar flux.

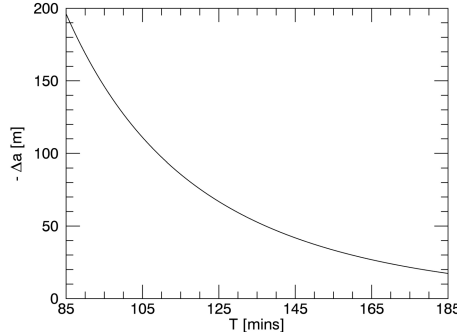


Fig. 5. Change of the semi-major axis with orbital period.

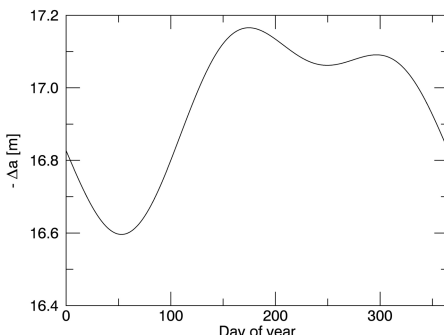


Fig. 6. Change of the semi-major axis during the one-year period.

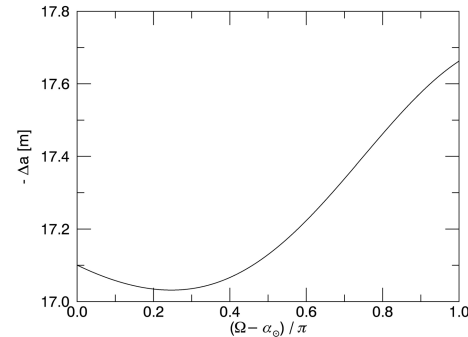


Fig. 7. Change of the semi-major axis with difference between right ascensions of the ascending node and the Sun.

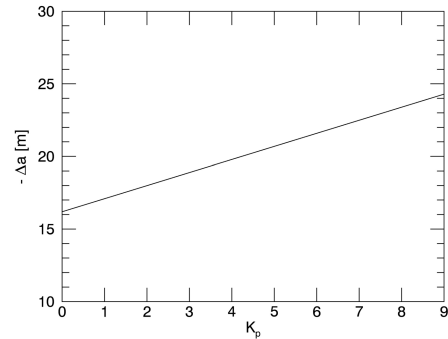


Fig. 8. Change of the semi-major axis with planetary K_p index.

figure, as well as the other ones shown in this section, is illustrative but not fully realistic due to the assumed constant value of eccentricity which is not the case in real missions.

On the other hand, the influence on Δa due to annual effects, the $\Omega - \alpha_\odot$ factor and planetary K_p index (Figs. 6-8) are for at least an order of magnitude less significant (on the scale of a single revolution) than the other ones listed above.

It is worth noting that execution of the code given here is up to 10 times faster compared to the classical approach with some of the iterative numerical integration methods. This feature enables eventual implementation of the code into the satellite software, providing quick and reliable real-time predictions of the orbit evolution.

5. CONCLUSION

The changes of a satellite orbit during one revolution are well described by the theory given by King-Hele (1964, 1987), which uses the total density as a factor that needs to be provided by the separate model. However, this procedure leads to complicated mathematical expressions that require numerical integration. In this work, we derive analytical forms by expanding the model terms into a series (up to

the second order) and then performing analytical integrations. The obtained expressions are, even though being very long with up to several hundreds of addends, given as sums of basic trigonometric and Bessel functions. As a result, we provide a very simple algorithm that saves majority of the processor time and energy, so it can be implemented into the satellite software, as well as online tools.

As the next milestone of the work in this field, we will provide analytical expressions for changes in the orbit eccentricity and inclination using the method given here. We will also elaborate methods for calculation of the drag coefficient depending on the satellite shape and orientation, thus extending the applicability to satellites with solar panels. Further on, we will create an online interactive tool that will be available to the community (on the basic and advanced user level) that will enable predicting of the orbit for any other future mission as well as comparison with already existing data.

Acknowledgements – Authors wish thank to the reviewer for constructive comments and helpful suggestions on an earlier version of the manuscript. The

first author was financially supported by the Ministry of Education and Science of the Republic of Serbia through the project 176002.

REFERENCES

- Bezdek, A. and Vokrouhlicky, D.: 2004, *Planet. Space Sci.*, **52**, 1233.
 Khalil, K. I. and Samwel, S. W.: 2016, *Space Res.* J., **9**, 1.
 King-Hele, D.: 1964, Theory of Satellite Orbits in an Atmosphere, Butterworth, London
 King-Hele, D.: 1987, Satellite orbits in an atmosphere. Theory and applications, Blackie and Son Ltd., Glasgow.
 Marčeta, D. and Šegan, S.: 2010, *Serb. Astron. J.*, **181**, 57.
 Milani, A., Nobili, A. M. and Farinella, P.: 1987, Non-gravitational perturbations and satellite geodesy, Adam Hilger Ltd., Bristol.
 Sehnal, L.: 1986, *Adv. Space Res.*, **6**, 151.
 Šegan, S.: 1988, *Celest. Mech.*, **41**, 381.
 Vallado, D.: 2001, Fundamentals of Astrodynamics and Applications, Microcosm Press, Portland

АНАЛИТИЧКИ ПРИСТУП МОДЕЛОВАЊУ УТИЦАЈА ОТПОРА АТМОСФЕРЕ НА ОРБИТЕ ЗЕМЉИНИХ ВЕШТАЧКИХ САТЕЛИТА

M. M. Martinović and S. D. Šegan

*Department of Astronomy, Faculty of Mathematics, University of Belgrade,
 Studentski trg 16, 11000 Belgrade, Serbia*

E-mail: mihailo.martinovic@obspm.fr

УДК 629.783 + 523.31-852
Претходно саопштење

Рад проучава промене у параметрима орбите Земљиних вештачких сателита услед утицаја отпора атмосфере. Како бисмо омогућили примену добијених резултата на будућим мисијама, дата је аналитичка интерпретација поремећаја путањских елемената са употребљивим или веома дугачким изразима. Такав развој је резултат избора посебног модела густине атмосфере. Коришћени модел

је TD88 са неким скорањима побољшањима на која је реферисано у тексту. Неки од израза и формула су изведені помоћу алгебарског софтвера *Mathematica* и тестирали у неким граничним случајевима. Резултати су показали задовољавајући ниво слагања са онима који су добијени користећи итеративни (нумерички) приступ.